PneuSleeve: In-fabric Multimodal Actuation and Sensing in a Soft, Compact, and Expressive Haptic Sleeve

Mengjia Zhu[1,2]**, Amirhossein H. Memar**[1]**, Aakar Gupta**[1]**, Majed Samad**[1]**, Priyanshu Agarwal**[1]**,**
Sean J. Keller[1]**, Nicholas Colonnese**[1]

[1]Facebook Reality Labs, Redmond, WA, USA, [2]University of California, Santa Barbara, CA, USA
mengjiazhu@ucsb.edu, amirmemar@fb.com, aakarg@fb.com, majed.samad@fb.com
pagarwal18@fb.com, seankeller@fb.com, ncolonnese@fb.com

ABSTRACT

Integration of soft haptic devices into garments can improve their usability and wearability for daily computing interactions. In this paper, we introduce *PneuSleeve*, a fabric-based, compact, and highly expressive forearm sleeve which can render a broad range of haptic stimuli including compression, skin stretch, and vibration. The haptic stimuli are generated by controlling pneumatic pressure inside embroidered stretchable tubes. The actuation configuration includes two compression actuators on the proximal and distal forearm, and four uniformly distributed linear actuators around and tangent to the forearm. Further, to ensure a suitable grip force, two soft mutual capacitance sensors are fabricated and integrated into the compression actuators, and a closed-loop force controller is implemented. We physically characterize the static and dynamic behavior of the actuators, as well as the performance of closed-loop control. We quantitatively evaluate the psychophysical characteristics of the six actuators in a set of user studies. Finally, we show the expressiveness of PneuSleeve by evaluating combined haptic stimuli using subjective assessments.

Author Keywords

Haptics; pneumatic actuation; wearables; closed-loop haptic rendering; vibration; compression; skin stretch; multimodal haptic display

CCS Concepts

•**Human-centered computing** → **Haptic devices;**
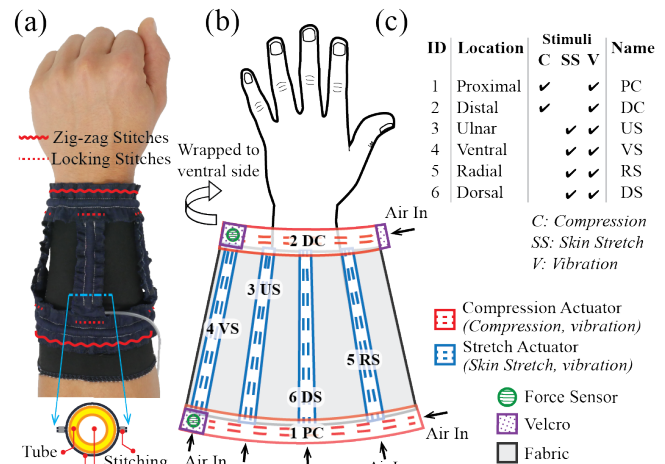
INTRODUCTION

We are in the midst of a mobile interface revolution. Developments in battery technology, capacitive touch screens, symbolic input algorithms, and ever growing computation power, have made smartphones ubiquitous. Similar recent developments in optics, display, tracking, and machine perception

Figure 1. PneuSleeve is a fabric sleeve capable of rendering complex combinations of compression, skin stretch, and vibration haptic stimuli to a user. (a) PneuSleeve prototype on forearm. Zig-zag stitches are used for integrating compression actuators with the sleeve substrate. Locking stitches are used for integrating stretch actuators with compression actuators. Lower insert illustrates the cross section of a single actuator. (b) PneuSleeve design consisting of six fluidic fabric muscle sheet actuators, two custom soft force sensors, a knit fabric sleeve base, and velcro connectors. (c) Actuation renderability of PneuSleeve. Compression actuators are used to provide compression stimuli and controlled grounding for skin stretch. All actuators can generate vibration stimuli.

are enabling the reinvention of mobile interfaces through augmented and virtual reality, AR/VR. Smartphone and head-mounted-display interfaces present complex and expressive visual and audio information, however, most widely-used interfaces capable of rendering haptic, or touch information today leave much to be desired in terms of wearability, and the haptic feedback they offer is often limited to simple vibrations. High-quality human computer interfaces should be capable of rendering a large set of complex and easily discernible haptic feedback, while also not encumbering the user. Ideally, these interfaces should seamlessly integrate into clothing or accessories that users already wear: jackets, shirts, bracelets, and so on.

Of all the possible wearable haptic interface locations, sleeve or armband devices offer several advantages. First, sleeves allow for a reasonable design space in terms of acceptable
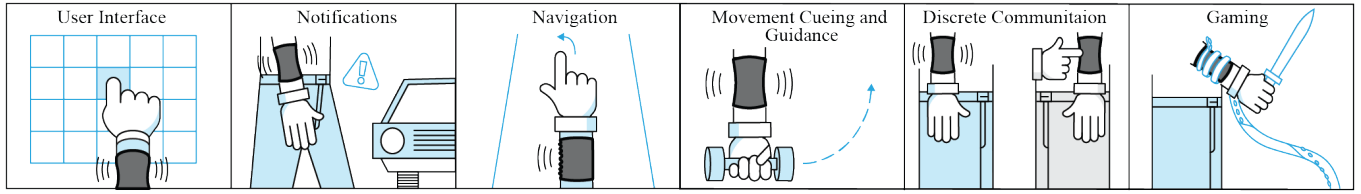
Figure 2. Paired with tracking and/or communication technology, the complex multimodal haptics of PneuSleeve enable a wide range of applications.

weight, size, power, and haptic renderable area, especially if heavier/bulkier components can be located elsewhere on the body. Secondly, sleeves leave the hands free, which is important to on-the-go AR scenarios as it allows the hands to manipulate the physical world unhindered. Finally, because shirts or jackets have sleeves, if the device can be integrated into normally-worn fabric, the device can be inconspicuous or even fashionable.

In this work, we created a lightweight fabric sleeve worn on a user's forearm *PneuSleeve*, that can render three distinct types of haptic feedback: compression around the arm, skin stretch tangent to the arm, and vibrations that result from high-frequency actuations of the compression and stretch actuators (Figure 1). By rendering combinations of these 'atomic' haptic stimuli in different locations and patterns in time, it is possible to communicate a large set of distinctly discernible and information rich haptic effects to the user. We hypothesize that coupling these haptic effects with audio/visual information can substantially increase the quality of a mobile human computer interface, particularly for uses in AR/VR (Figure 2).

In this paper, we make the following contributions:

- The design and construction of a novel fabric sleeve embedded with six soft pneumatic actuators and two customized mutual capacitance sensors. The actuators enable complex combinations of compression, skin stretch, and vibration. The two soft sensors enable closed-loop regulation of compression force.

- Physical characterizations for the a) quasi-static and transient performance of the actuator, b) resolution and consistency of the sensor, and c) performance of the closed-loop compression force control system.

- Psychophysical characterization of the absolute detection thresholds (ADTs) and the just-noticeable differences (JNDs) of the six actuators in PneuSleeve.

- Subjective assessments of 23 feel effects that demonstrate PneuSleeve's rich expression capability.

RELATED WORK

In recent years, buoyed by developments in AR/VR, there has been a dramatic increase in interest and production of mobile, wearable, haptic interfaces. We present an abbreviated list of wearable haptic interfaces in Table 1. In this paper, we focus on related work for wearable haptic interfaces, and do not emphasize related work in handhelds/holdables . Wearable haptic interfaces have been implemented on many different locations

on the body, where thimbles, gloves, bracelets, sleeves, and jackets, are the most popular.

Thimbles
Thimbles stimulate a user's fingertip, which is one of the most sensitive parts of the human body, and is often involved in probing or manipulating the environment. They can provide salient and useful haptic stimuli, however, most current thimble interfaces are bulky and do not allow interaction with physical objects. Pacchierotti et al. present a survey of over twenty thimble interfaces rendering variations of normal compression, lateral skin stretch, and vibration [15]. Most thimbles use electrically powered direct current or servo motors to position a rigid plate or tactor on the fingertip [22, 20].

Gloves
Gloves are capable of rendering haptic feedback to the entire hand, and may one day allow direct manipulation with virtual objects. However, current designs face a number of challenges regarding encumbrance, locating actuators, grounding forces, and power requirements. Pacchierotti et al. present a survey of over twenty glove interfaces rendering various haptic stimuli [15]. Similar to thimbles, most glove interfaces are powered electronically and use direct current or servo motor actuators. Notable 'soft' gloves using different actuation approaches are thin form factor electrostatic brakes [10] or molded elastomeric chambers with fiber reinforcements [19]. Takahashi et al. used pneumatic actuators for glove fitting and finger posture control [26], however, multi-modal actuation with user specific control methods was not implemented in their studies.

Bracelets
Bracelets are socially acceptable and leave the user's hands free to interact with the physical world. Huang et al. used sixteen servo motors and taxels to render virtual objects with deformable rear-surfaces [11]. Pezent et al. presented a multisensory squeeze and vibrotactile bracelet using one servo motor and six linear resonant actuator vibrotactors [17]. Shim et al. developed another multimodal tactile display using wind and vibration [24]. A brushing stimulation bracelet was presented in [25], and a thermal one in [16]. Shear forces and motion rendering have also been explored in Whitmire et al.'s work [29].The majority of presented bracelets are often 'hard', created using rigid components, such as thermosets, motors, metals, and so on. However, there have been some 'soft' bracelets created using low stiffness, flexible, and stretchable components, like fabric or elastomers explored in recent years. To achieve squeeze sensation, Gupta et al, configured shape memory alloys (SMAs) around wrist [7], while Pohl et al. chose blood pressure cuffs [18]. Other multi-modal haptic

Haptic Stimuli: C = compression, SS = skin stretch, V = vibration, T = temperature, I = impedance. Actuators/Sensors: LRA = linear resonant actuator, TPU = thermoplastic polyurethane, SMA = shape memory alloy, PU = polyurethane, ERM = eccentric mass motor, cap. = mutual capacitance, FSR = force sensitive resistor.

	Form Factor	Power Source	Actuator Design	Sensor Type	Haptic Stimuli				
					C	SS	V	T	I
Zhu, 2020 (this work)	sleeve	pneumatic	tube in fabric	cap.	✓	✓	✓		
Pezent [17], 2019	bracelet	electric	motor, LRA	encoder	✓		✓		
Young [31], 2019	bracelet	pneumatic	TPU bellow		✓		✓		
Peiris [16], 2019	bracelet	electric	peltier, piezo	temp.				✓	
Hamdan [8], 2019	variable	electric	multi-layer SMA			✓			
Delazio [4], 2018	jacket	pneumatic	PU bladder	FSR	✓		✓		
Hinchet [10], 2018	glove	electric	electro-static brake	vision					✓
Raitor [21], 2017	bracelet	pneumatic	TPU bladder			✓			
Gupta [7], 2017	bracelet	electric	SMA			✓			
Pohl [18], 2017	bracelet	pneumatic	air cuff	pressure					✓
Schorr [22], 2017	thimble	electric	motor	encoder	✓	✓			
Polygerinos [19], 2015	glove	hydraulic	fiber in elastomer	pressure					✓
Tang [27], 2014	sleeve	electric	ERM, LRA	pressure			✓		
Prattichizzo [20], 2013	thimble	electric	motors	encoder	✓	✓			
Bark [3], 2009	sleeve	electric	motors	hall effect		✓			

Table 1. Abbreviated List of Wearable Haptic Interfaces

stimulations combining local pressure and vibration have also been explored in Young et al.'s work [31]. These devices are soft to wear, but few combines actuation modalities include compression, vibration and skin stretch, limiting the expressiveness that one device may render.

Sleeves
Sleeves have similar advantages and disadvantages in wearable haptics to bracelets. Relative to bracelets, they present a larger renderable area, but can be more challenging to fit a diverse set of users. Tang et al. presented a sleeve composed of a grid of rigid vibrotactile actuators for treating autism [27]. Bark et al. evaluated an armband that renders skin stretch using an ultrasonic motor and cable transmission [3]. Ion et al. explored another armband that renders 'skin drag' using rigid components and an electric motor [12]. In Agharese et al.'s work, a soft forearm interface that grows to wraps along the users arm using pneumatic pressure was invented [1]. Hamdan et al. used multi-layer shape memory alloys (SMAs) to render various haptic stimuli based on linear extension or contraction. The connection to the user is a 'skin sticker' that can attach to the forearm as well as other locations. In addition, multiple pneumatic actuators have been integrated into a sleeve to create the illusion of lateral motion on the arm [30].

Jackets
Jackets present a large haptic renderable area, but face challenges in complexity, size/weight, and coupling to the human for effective transmission of haptic stimuli. Delazio et al. presented a jacket with pneumatic airbag actuators and force sensors to increase realism [4]. Arafsha et al. presented a jacket

with vibration and temperature haptic actuators to enhance emotional immersion [2]. Foo et al. used SMAs to explore user experiences of garment-based dynamic compression [5].

DESIGN OF PNEUSLEEVE SYSTEM

Soft Actuator Design
'Soft' haptic interaction devices created from composite structures of fabrics or elastomers have a key advantage over 'hard' devices created from rigid metals or thermosets: soft devices feature a smaller difference in mechanical impedance between the device and human, allowing for better fit, leading to more efficient sensing and transmission of haptic stimuli.

For this reason, we use Fluidic Fabric Muscle Sheets (FFMS) [32] as the actuator in PneuSleeve. FFMS actuators operate as inverse pneumatic artificial muscles (IPAMs) [9], where at high fluid pressure the actuator is in its longest state. As the pressure decreases, the actuator contracts and exerts force on the blocking element. Therefore, IPAMs can be used as either a linear, or compression actuator when wrapped around an object [32]. Contrary to McKibben muscles [23, 6] that shorten in accordance with a radial expansion, FFMS actuators change length without expanding radially. This characteristic enables them to have low profile during operation, eliminating unwanted parasitic forces generated by radial expansion of the actuator. Compared to Share Memory Alloy (SMA) actuators [8], which contract and lengthen due to a thermally activated phase change, FFMS actuators feature faster response times without generating any unwanted thermal stimuli.
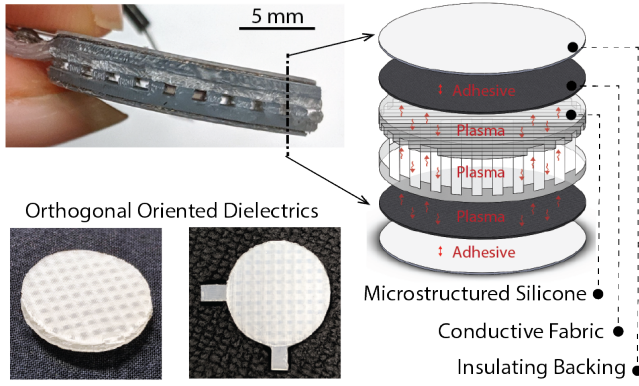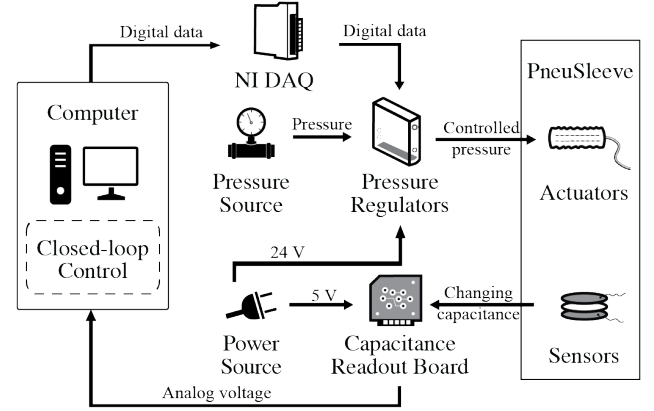
Figure 3. Customized mutual capacitance sensor to measure force. Two silicone dielectric layers with microgrooves are oriented orthogonally between conductive fabrics to increase sensitivity. Plasma treatment is used to bond interfaces between silicone layers and conductive fabrics.

Figure 4. PneuSleeve system architecture using measured capacitance from the sensor as the feedback for the closed-loop control of the actuator compression force.

PneuSleeve consists of six single-channel pneumatic FFMS actuators: two provide radial compression on the proximal and distal forearm, and the other four generate linear stretch at ulnar, radial, ventral, and dorsal side of the forearm. All actuators can render vibration (Figure 1). For linear stretch actuation, all six actuators are pressurized to their longest length. Compression actuators are first compressed to provide grounding or anchoring force for the linear stretch actuators. Then, the linear stretch actuator shortens and moves the connection points with the already compressed compression actuators, thus generating effective localized compressive shear on the skin. When the actuator is pressurized back, the skin recovers to its normal state due to its own elasticity to render extensive shear. Due to the soft nature of the actuator and fabric, occasional actuator touch with the passive sleeve is not noticeable compared to the sensation of the skin stretch. The skin stretch sensation is dominated by large deformations caused by shortening the actuators, rather than the sensation caused by bunching and releasing of the actuator.

The six FFMS actuators are fabricated using the method described in [32]. Latex tubes with outer diameter of 5.5 mm and wall thickness of 0.5 mm are used as the stretchable tubings. Non-stretch woven fabrics with straight stitching are used to construct conduits with 7.5 mm width for constraining radial expansion of the soft tubes. The lengths of the stitching for distal compression, proximal compression, and stretch actuators are 250 mm, 170 mm, and 80 mm, respectively. After inserting the tubings, the conduits are all wrinkled to 40% of their original length. Finally a barbed tube fitting is attached to the end of each latex tubing. The cross section of a single actuator is shown in Figure 1(a) lower insert.

Soft Mutual Capacitance Sensor Design

To render high-quality haptic feedback, it is important to prevent the slippage of compression actuators and maintain a suitable grounding force when skin stretch actuators are activated. Therefore, we implement a closed-loop controller to regulate grounding compression forces to users with different forearm sizes and anatomies. This control is enabled by a soft force

sensor based upon sensing mutual capacitance. We choose capacitance sensing over force sensing resistors due to its low temperature sensitivity. The capacitance C of a parallel-plate capacitor is inversely proportional to the distance d between the parallel plates when the permittivity ε and the electrode area A are constant ($C = \varepsilon * A/d$). A change in the compression force results in a change in the gap between the electrodes and accordingly a change in the capacitance.

Based on the capacitance sensing theory, we use a layered structure of dielectrics, electrodes and insulators for the sensor (Figure 3). The transfer function between the capacitance and the applied force (compression force generated by the actuator in our case) is heavily dependent on the stress-strain behavior of the dielectric material. Two main performance characteristics, hysteresis and relative capacitance change ($\frac{\Delta C}{C_0}$, where C_0 is the capacitance baseline) are considered to select sensor material and geometry.

To find the most suitable dielectric materials for PneuSleeve, a variety of dielectric films including foams, 3D printed Elastomeric Polyurethane (EPU) with microgrooves and pillars, and 3D molded silicone with microgrooves [33] are fabricated and tested. Due to the small applied force (about 4 N according to Figure 6), microstructures are used to increase the relative capacitance change of the sensor. Among explored dielectrics, foams show a high relative capacitance change with large hysteresis, while 3D printed EPU dielectrics reveal low hysteresis but low relative capacitance change. 3D molded silicone dielectrics with microgrooves are finally selected due to their low hysteresis and good relative change of capacitance (12% over the compression forces , Figure 8). Conductive fabrics are chosen as the electrodes due to their flexibility that ensures uniform layer bonding with the dielectrics. The overall shape of the sensor is designed to be circular to avoid the edge effect on the electric field caused by sharp corners.

The dielectrics are fabricated by casting Ecoflex 00-30 in a 3D printed acrylic styrene acrylonitrile (ASA) mold with microgrooves of width 1 mm, periodic width 2mm, and height 0.75 mm. Ecoflex 00-30 is mixed and degassed before pour-
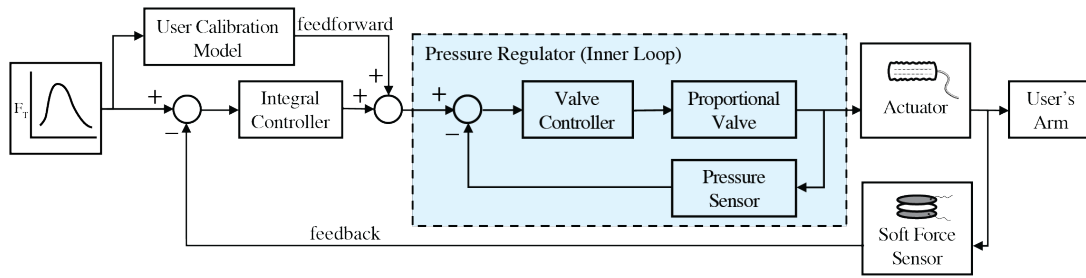
Figure 5. Block diagram of the closed-loop control regulating compression force to the user. The highlighted inner loop is embedded into the pressure regulator to reach the commanded pressure signal. The user's calibration model is used for feedforward, and an integral controller using the soft force sensor measurement is used for feedback.

ing into the mold, then cured at 80°C for 1 hr. Two layers of the molded dielectrics are plasma treated and bonded orthogonal to each other. Plasma treatment is also used to bond the conductive fabrics with 0.1 mm thickness to the dielectrics. Finally, acetal sheets with 0.2 mm thickness are used as the insulating layers for the electrodes with double-sided adhesives. The total thickness of the sensor is 3.9 mm.

Wearable Sleeve Design
A highly elastic knit fabric base and Velcros are used to configure a sleeve form-factor combining the chosen actuator and sensor designs (Figure 1(b)). Velcro patches are sewn on the ends of compression actuators for radial closure and safety quick release. Sensors are placed underneath the Velcro patches on the compression actuators. All actuators are fully pressurized (200 kPa) and assembled on the fabric sleeve base using zig-zag stitches to maintain the stretchability and flexibility of the sleeve and the actuators. The connection between the ends of the stretch actuators and the the edges of the compression actuators are then reinforced with locking stitches (Figure 1(a)). The constructed sleeve has a total weight of 26 grams and a maximum thickness of 6 mm. With fabric as the basic construction material for the pneumatic actuators and sensors, PneuSleeve is intrinsically soft, low profile, and can be easily donned and doffed.

Pneumatic Control System
PneuSleeve has six pneumatic actuators and two mutual capacitance sensors. Each pneumatic actuator is controlled through an individual pressure regulator (Festo VEAB, 1-200 kPa) (Figure 4). The pressure regulators are proportional control three-way valves that have inlet, outlet, and exhaust ports. The air is vented to the environment and the inlet is connected to a compressed air reservoir. Each pressure regulator is controlled using an analog output generated through a data acquisition device (NI cDAQ-9174 with NI9264 module) interfaced using a PC. The capacitance of the soft force sensor is measured through a custom-built capacitance sensing board. The measured capacitance acts as the feedback for the closed-loop control of the actuator compression force.

Closed-Loop Force Control
Using the real-time force feedback from the integrated soft sensor, we implement a closed-loop control strategy to apply user-specific grounding forces. Figure 5 shows the block diagram

of the closed-loop controller. The outer feedback loop controls the compression force, which is rendered to the user by generating pressure commands to the pressure regulator. The control architecture uses a personalized calibration model to approximate the pressure-force map as a feedforward term, and employs an integral controller for its feedback loop. The calibration model improves the convergence speed of the controller and it is built once for each user after putting on the sleeve. The calibration process is conducted by deflating and inflating the compression actuators from 200 kPa to atmosphere pressure. A third degree polynomial is then fitted to the recorded data to serve as the feedforward function. The inner loop is embedded in the pressure regulator to reach the commanded pressure using its internal pressure sensor and embedded controller.

Noise Management
The noise in pneumatic systems mostly comes from switching action of the pressure regulators, and venting of the high pressure air to exhaust. In our system, the Festo proportional pressure regulators has a 'silent operation' feature based on piezo technology, which uses control frequencies above the human hearing range. To reduce the air exhaust noise, an off-the-shelf muffler is used on the regulator's exhaust port. With this arrangement, the noise for most haptic actuation in our study can be barely heard without headphones.

PHYSICAL CHARACTERIZATION AND EVALUATION
Quasi-Static Characterization
To characterize the relationship between pressure, force and the length of the FFMS actuator, a set of quasi-static experiments are conducted. A force sensor (ATI Nano 17) is used to measure actuator tension force as a function of input pressure controlled by a pressure regulator (Figure 6 inserts). A motorized linear stage is used to adjust the distance between the two ends of the actuator before the loading and unloading test of the actuator. A deflation-inflation cycle (200 kPa to atmosphere), with a duration of 40 s is performed on the actuator for discrete actuator lengths with a 4 mm step size (ΔL). Figure 6 shows the pressure-force curves for 5 discrete distances between the endpoints of the actuator (L). According to the functional principle of FFMS actuators, for a given pressure the actuator force decreases as L shortens [32]. The observed hysteresis effect between loading and unloading curves is mainly due to the friction between the stretchable tubing and the fabric to which it is embroidered.
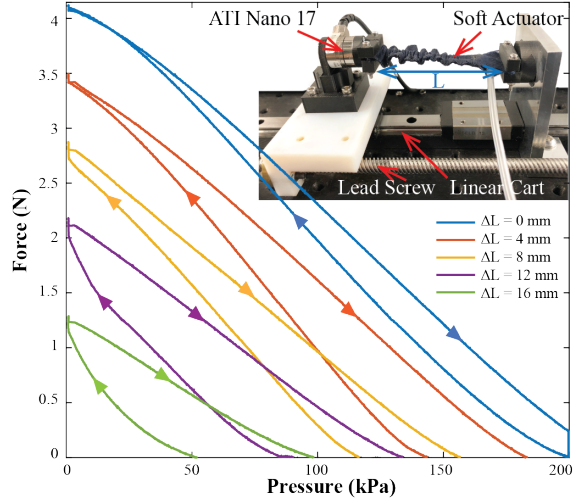
Figure 6. The results of the characterization tests. Each curve corresponds to a deflation and inflation cycle at a certain displacement of the actuator endpoint. L_0 **is the length of the actuator at high pressure (200 kPa) and** $\Delta L = L_0 - L$ **denotes the change in the actuator end-point position. The arrows on the curves indicate the deflation and inflation cycles.** *Inserts:* **Actuator characterization setup for quasi-static analysis.**

Figure 7. Frequency response of the compression actuator for different amplitudes. Frequency axis is in log scale from 1 Hz to 50 Hz. The red dots represent the magnitude determined using the experimental data, and the lines represents a fitted spline to the experimental data. *Inserts:* **Dynamic response characterization setup for the compression actuator.**

Dynamic Frequency Response

To generate vibrations at each actuator location, the actuation needs to work at high frequencies. As the frequency of actuation becomes higher, the rendered force magnitude will be reduced due to the compressibility of air and shorter fill and drain cycles. The frequency response of an actuator provides the force magnitude that the actuator is able to render at a given frequency. A frequency response characterization is conducted for the radial compression actuator using a test setup with a force sensor (ATI Nano 17) (Figure 7 inserts). A set of sinusoidal input pressure at different frequencies (1 to 50 Hz divided into 20 equidistant steps using logarithmic spacing) is commanded to the actuator for 50 cycles each, and resulting compression force response are measured for each frequency. A fast-Fourier transform analysis is conducted on the commanded pressure data and the measured compression force data for each frequency. The force-frequency response is obtained by dividing the output amplitude corresponding to each commanded frequency with the respective input amplitude. The input signal is also normalized with the amplitude of the sinusoidal signal to obtain the frequency response in the units of force. This characterization is repeated at different amplitudes of the sinusoidal input pressure. Results indicate that the force magnitude reduces with increasing input frequency. Furthermore, with higher pressure amplitudes higher force magnitude can be achieved for a broader frequency range. This is primarily due to the way internal controller of the pressure regulator functions. Although the force magnitude attenuates with the increased frequency, an easily perceptible force of 50 mN can be achieved at 20 Hz (Figure 7).

Sensor characterization

To obtain the transfer function of the capacitance sensor, the compression testing setup for dynamic characterization is
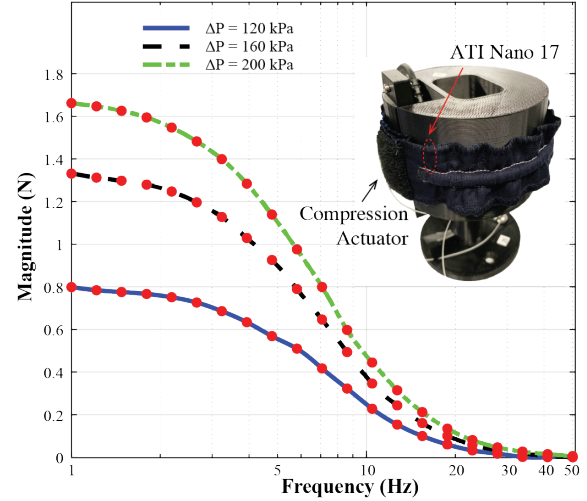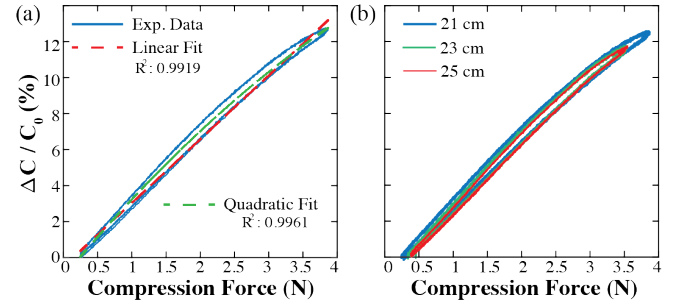

Figure 8. (a) Experimental data and fitted models relating measured capacitance to compression force. (b) Experimental data for various cylinder circumferences showing consistent behavior. The unloaded capacitance, C_0**, is 6.6 pF.**

adopted (Figure 7 inserts). The pneumatic pressure is linearly varied between 200 kPa and atmosphere pressure in a duration of 40 s for 5 cycles. Capacitance output of the sensor for all 5 cycles are highly consistent (Figure 8 (a)), with more than 12% relative change in capacitance under the force applied by the actuator, and a small hysteresis. A linear fit is sufficient to capture the variance of the data with R^2 of 0.9919. To further improve the accuracy, quadratic fit is used as the transfer function between compression force and capacitance.

In addition to the hysteresis and relative capacitance change, the curvature of the forearm on different users may cause inconsistent output from the sensor. Therefore, we examined the consistency of the sensor on a set of surfaces with different curvatures. These curvatures are generated by using the cylinders in the compression setup with different circumferences (21 cm, 23 cm, and 25 cm). The results indicate that the capacitance outputs among cylinders with different circumferences are highly consistent (Figure 8 (b)). Although in
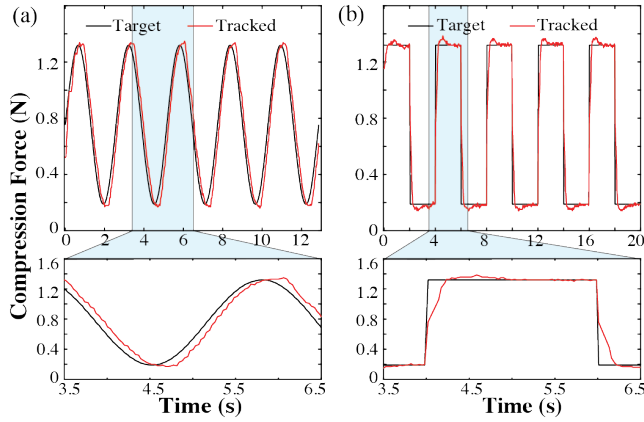
Figure 9. Closed-loop control performance for a commanded sinusoidal, (a), and squared, (b), compression force. The black line indicates the desired compression force profile over time and the red line shows the tracking performance recorded from the soft force sensor on the user's arm. The root-mean-square tracking error for the sinusoidal input was 0.10 N, and the settling time for squared input was less than 0.3 s.

practice user's arms are not rigid, results demonstrate that the transfer function does not change significantly with varying arm circumferences.

Closed-Loop Control Response

To evaluate the performance of the proposed control method (Figure 5), two different types of input force profiles (F_T), including sinusoidal and squared waves, were fed to the controller while the PneuSleeve was worn by a user and tracking results were recorded. The outer control loop was set to operate at 40 Hz and the integral controller gain was set to -0.025. Considering the compressability of the air, the tracking error and response time results indicate the suitable performance of the controller for a soft wearable actuator (Figure 9).

USER STUDY: PSYCHOPHYSICAL EVALUATION

The aim of the user study is to evaluate the perceptual characteristics of the 'atomic' haptic cues provided by the PneuSleeve. Primarily, we seek to evaluate the absolute detection threshold (ADT) for compression and skin stretch actuators, as well as the just-noticeable difference (JND) for those same cues. In the following sections, we will refer to these haptic cues generically as 'the stimulus,' which will be either compression or skin stretch depending on the corresponding actuator. Since the actuators are their longest at high pressure, and contact and exert forces as the pressure decreases, for simplicity, the stimulus levels are reported in terms of $\Delta P = P_H - P$, where P_H is maximum pressure (200 kPa) and P is the variable controlled pressure.

Absolute Detection Threshold (ADT) Evaluations

We conducted ADT evaluations for the two compression actuators and the four skin stretch actuators to understand the minimum pressure required for the user to feel those sensations. We conducted a standard two-down, one-up adaptive staircase procedure in order to estimate the 71% threshold. Every stimulus was applied for a duration of 1 s. The experiment started with

a stimulus of 0 kPa. For every stimulus that was not felt, the stimulus was increased by a step size of 20 kPa, and increased by the same if the stimulus was felt twice consecutively. After three reversals, the step size was changed to 2 kPa. The experiment ended after nine total reversals and the average from the last five was taken as the threshold estimate. The high initial step size of 20 kPa ensured quick jumps to the ADT vicinity thus minimizing total number of trials, after which the smaller 2 kPa step size ensured convergence to a fine-grained value.

Twelve participants (six female, six male, ages 24–34, mean = 28.5, all right-handed) took part. We recorded the arm circumferences near the distal compression actuator (range: 13.7–18 cm, mean = 15.5 cm) and the proximal compression actuator (range: 19.9–25.7 cm, mean = 22.2 cm). Participants wore the sleeve on their left forearm with the arm resting on a table and hidden from their view during the study using a box. Participants wore active noise canceling headphones playing Pink noise for complete sound insulation. The ordering of the six ADT estimation staircases (1 for each actuator) was randomized. Participants responded 'Felt' or 'Not Felt' by pressing the corresponding keyboard key after every stimulus. A random interval of 2–6 seconds between the participant's response and the next stimulus was introduced to minimize anticipation of the stimulus at a particular instant.

Just-Noticeable Difference (JND) Evaluations

We conducted JND evaluations for the two compression actuators and the four skin stretch actuators. Prior work has shown that haptic sensations including pressure [18, 7] generally follow Weber's law. We therefore conducted the JND using a single reference value, which demonstrates that users are able to discriminate certain intensities in PneuSleeve actuators. The same participants from the ADT study did the JND study in the same session with the complete study taking about an hour. The reference stimulus was chosen to be 1.3 times the participant's ADT. This normalizes the reference across all participants with regards to its perceived intensity. This is also preferable with respect to using a constant pressure value since depending on the arm size and stiffness, the same pressure may result in different forces on different users and the reference stimulus may perceived differently.

We used a three-down, one-up adaptive staircase procedure to estimate the JND with participants performing a two-interval forced choice, thus targeting the 79% threshold. For every trial, participants were presented with a pair of stimuli appearing one after the other, and they judged which one felt stronger. Each pair consisted of the reference stimulus (R) and offset stimulus ($R + \Delta$). Every stimulus was applied for 1 s, and the ordering of reference and offset stimuli within a trial was randomized. The experiment started with a large offset value (Δ) of 100 kPa. For every sequence of three correct responses, the offset was decreased by a step size of 48 kPa, and increased by the same upon a single incorrect response. After two reversals, the step size was changed to 4 kPa. The experiment ended after eight total reversals and the average from the last four was taken as the JND estimate. The experiment design was finalized after initial pilots to optimize the accurate estimation of JND and the duration of the experiment.
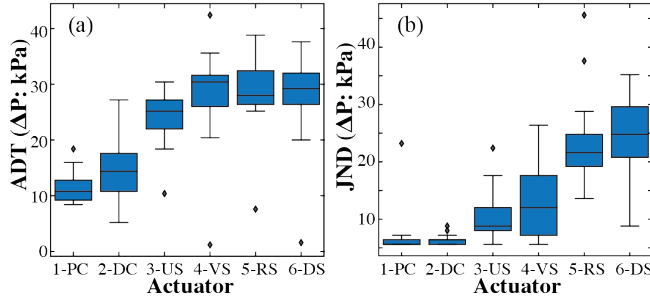
Figure 10. ADTs, (a), and JNDs, (b) for all six actuators embedded in PneuSleeve (Figure 1) in terms of $\Delta P = P_H - P$, with initial pressure P_H =200 kPa. The detectability and sensitivity differences may be attributed to the type and location of the actuator.

ADT and JND Results Discussion

The box plots of Figure 10 show the distribution of the estimated ADT and JNDs with the whiskers representing first and third quartiles. The results show that thresholds are lower for the compression actuators than for the skin stretch actuators, indicating that users are more sensitive to the sensations produced by the compression actuators. We also observe a higher variability in the JND estimates for the stretch actuators which is consistent with the reduced sensitivity to those actuators. However, interestingly, the estimated values of the JND for all actuators is well smaller than maximum possible ΔP that it is possible to actuate ($\sim$20 kPa as compared to 200 kPa). This is about one order of magnitude below the full range, plausibly providing for between 5 and 10 distinctly perceivable levels, depending on the exact Weber fraction for these sensations.

USER STUDY: FEEL EFFECTS

Our psychophysics studies establish that PneuSleeve can stimulate varying magnitudes of compression and stretch pertaining to the six actuators. As mentioned earlier, PneuSleeve can also stimulate vibrations by actuating at higher frequencies. Here we demonstrate the expressivity of PneuSleeve using a vocabulary of 23 feel effects designed by a haptics researcher that are based on various spatio-temporal combinations of compression, stretch, and vibrations. Prior work has conducted similar feel effects studies [4, 14]. We follow a design similar to Delazio et al. [4] to see if users perceive the sensations to be good fits for their descriptions and whether they like the feeling or not. The feel effects correspond to different real-world use-cases classified into seven families as shown in Table 2.

Design of Control Signals

In practice, any signals in time series can be used as control signals for the air pressure. To form a design method for PneuSleeve, single actuator response design and combined actuation design are chosen as the two main design considerations. Single actuator response design includes the design of the waveform for a single actuation cycle, duration of the waveform, number of repeated cycles, and the time gap in between repeated cycles. The main attribution to different haptic sensations is the characteristics of the single-cycle waveform. Sinusoidal and square waves were used as the basic units to construct the waveform. Frequency, amplitude, and duty cycle

Family	Feel Effect	Haptic Stimuli			Force Control	Active Actuators
		C	SS	V		
Accel-eration	Acceleration	✓		✓	N	1, 2
	Deacceleration	✓		✓	N	1, 2
Rotation	Continuous rotation - CW	✓	✓	✓	Y	All
	Continuous rotation - CCW	✓	✓	✓	Y	All
	Discrete rotation - CW	✓	✓		Y	All
	Discrete rotation - CCW	✓	✓		Y	All
Heart-beat	Normal heartbeat	✓		✓	N	1, 2
	Racing heartbeat	✓		✓	N	1, 2
Navi-gation	Back to front direction	✓		✓	N	1, 2
	Front to back direction	✓		✓	N	1, 2
	Bottom to top direction	✓	✓	✓	Y	1, 2, 4, 6
	Top to bottom direction	✓	✓	✓	Y	1, 2, 4, 6
	Left to right direction	✓	✓	✓	Y	1, 2, 3, 5
	Right to left direction	✓	✓	✓	Y	1, 2, 3, 5
Phone	Phone alarm	✓	✓	✓	N	All
	Phone notification	✓		✓	N	1, 2
Waves	Forward and backward waves	✓			N	1, 2
	Left and right waves	✓	✓		Y	1, 2, 3, 5
	Top and bottom waves	✓	✓		Y	1, 2, 4, 6
Special Effects	Spring	✓	✓		Y	All
	Snake crawling	✓	✓		Y	All
	Underwater	✓			N	1, 2
	Breathing	✓			N	1, 2

Table 2. List of the 23 feel effects tested in the subjective user study. Feel effects are grouped into 'families' based on the similarity of their control signals. C = compression, SS = skin stretch, V = vibration, CW = clockwise, CCW = counterclockwise.

can be controlled for fine tuning the effects. Combined actuation considerations include the selection of the actuators, the sequence of actuation, the phase shift, time lagging, and overlapping of signals in between selected actuators.

With these design factors, we composed 23 feel effects and grouped them into seven families based on the similarity of their control signals (Table 2 and Figure 11). Acceleration family features a linear change in sinusoidal frequency of the compression actuators. Rotation signals feature the sequenced actuation of the stretch actuators. The difference between continuous and discrete rotation is that continuous rotations are vibration-based. The latency of switching from one stretch actuator to the next are the same for both. Heartbeat signals have fine-tuned magnitude and delay time on two compression actuators. Navigation cues feature an overlap on the signals between actuators to make the transition smoother. Phone alarm uses long duration vibration on all six actuators at the same time intended to grab more attention from user, while phone notification has two short vibrations on two compression actuators. Waves and special effects family signals are constructed on sinusoidal waveforms with frequency less than 0.5 Hz. Opposite phase between active actuators is used in waves, while shifted phase and same phase are used in special effects, with shifted phase implemented in underwater, and snake crawling, and same phase implemented in spring and breathing. In addition to the phase difference, the active actuators are also selected differently for different effects. A grounding force of 0.5 N is used on compression rings for corresponding effects requiring controlled grounding as listed in Table 2.
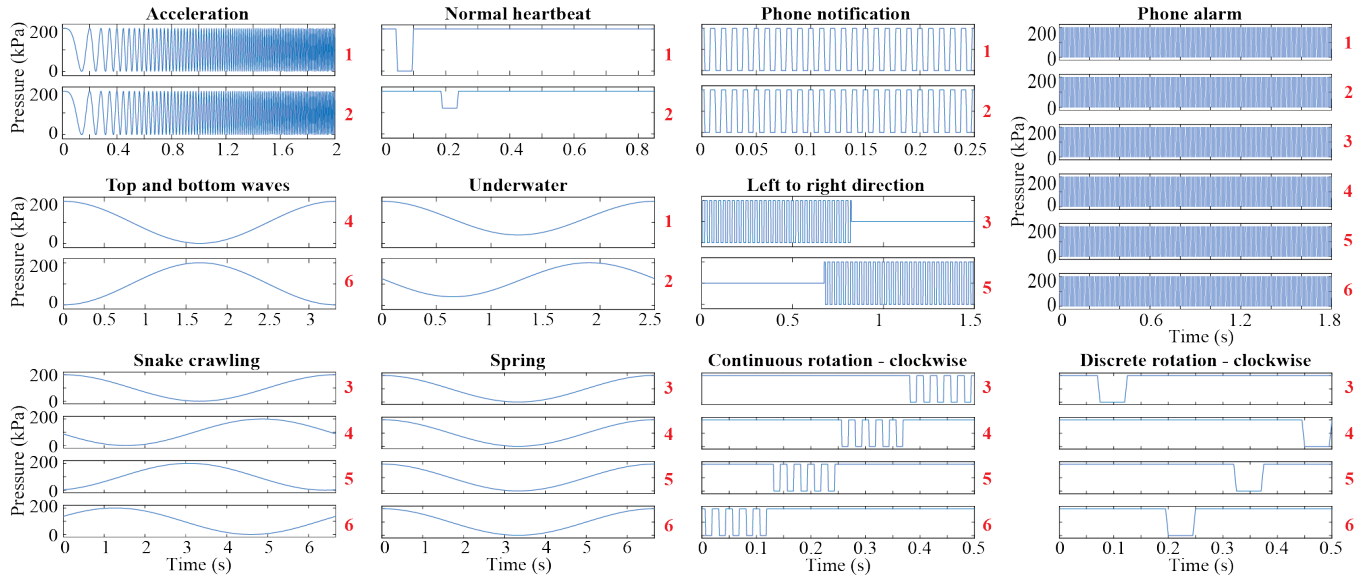
Figure 11. Example single-cycle control signals for selected feel effects. Bold red numbers denote the index of the active actuator (Figure 1).
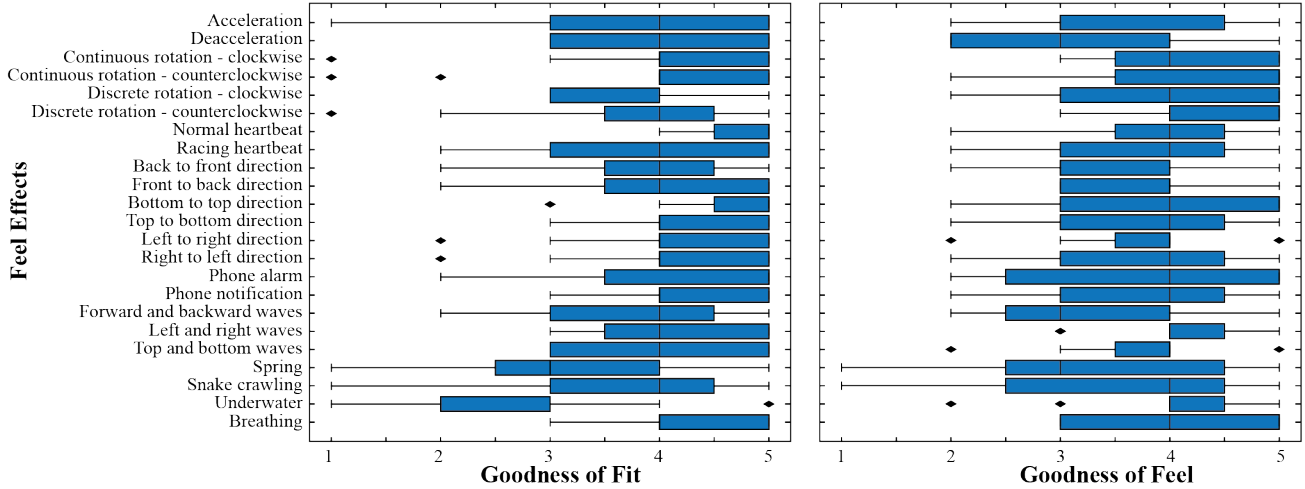

Figure 12. Box plots showing the Goodness of Fit and Goodness of Feel ratings for the 23 feel effects.

Evaluation Methods

We validate these feel effects in a user study along two axes: 'Goodness of Fit' and 'Goodness of Feel'. Goodness of Fit indicates how well the haptic sensations fit the name of the feel effect. Goodness of Feel indicates how well the sensation feels regardless of whether it is a good fit for the feel effect.

Eleven participants (five female, ages 26–46, mean = 31.6, 10 right-handed) participated. We recorded the arm circumferences near the distal compression actuator (range: 13.7–18 cm, mean = 15.9 cm) and the proximal compression actuator (range: 19.9–25.7 cm, mean = 22.8 cm). The feel effects were grouped into families and the ordering of the families and feel effects within the families were both randomized. The goodness metrics were explained to the participants. For each effect, participants were asked to rate the goodness of fit and feel on Likert scales of 1-5. Participants were allowed to play

an effect as many number of times before their response. Participants were asked for feedback on their perceptions after each family of effects was completed.

Feel Effects Study Results and Discussion

Figure 12 shows that participants rated most feel effects high for both goodness of fit and feel. Participants found the sleeve to be comfortable overall. Multiple participants commented on liking the soft sleeve form factor. According to P3: *'No hard material, others feel like watch, this is like a sleeve, so light weight, very nice feeling.'* Participants also compared the vibration sensations to regular vibrotactile feedback. P1: *'With the watch vibrations there is a slight shock. The vibrations here are like light touch, they feel good.'* Participants also found the vibration based rotations to be a better fit than discrete stretch based rotations. Given that prior works have shown that sequenced vibration on the skin can lead to a feeling

of apparent motion [13], the preference for vibration based rotation is reasonable.

Participants were divided on the feel of sensations which relied on strong squeeze effects, especially the deceleration, forward-backward waves, and spring. P7: *'The deceleration feels too strong initially. It reminds me of when I'm getting my blood pressure done.'* Participants had similar comments about the phone alarm, where they felt it was too strong, especially since it was actuating all the actuators simultaneously. P5: *'I like the pattern: very similar to an alarm but it's too strong. I guess an alarm is supposed to grab attention, so I think it's perfect in that sense.'*

Participants also came up with alternate interpretations of the sensations, likening the racing heartbeat to a galloping horse, the spring loading and unloading to rolling and unrolling of an arm sleeve, and the discrete rotations to an old train. One participant who was a gamer indicated the importance of context in the interpretation of these sensations. P10: *'I can imagine these sensations being useful in racing games, shooting games, also in virtual reality.'* Multiple participants alluded to applications for remote touch or emotion communication. P6: *'You can almost imagine the alarm as an angry squeeze from someone.'* P10: *'Instead of underwater, it feels more like somebody is massaging or kneading your arm.'* P8: *'It (breathing sensation) feels like a baby breathing in your arm. It's relaxing.'*

LIMITATIONS AND FUTURE WORK
Our results indicate that PneuSleeve is a promising initial step toward soft multimodal haptic interfaces. However, there are several limitations and opportunities for further development. PneuSleeve is controlled using pneumatic pressure and features a compressed air reservoir for a power source and pressure regulators for individual activation. Although flexibility and mobility can be achieved by using long air tubes, the current apparatus has limited portability. This could be achieved with the advances in microelectromechanical systems and chemical engineering [28].

Our psychophysical and feel effects studies indicate that PneuSleeve is capable of rendering a rich vocabulary of different haptic effects. This opens the door for explorations on sensory substitution or augmentation studies using PneuSleeve. For the compression actuators, sensory masking may occur after some duration of stimulus and is an avenue worth investigating. Our work focuses on the haptic rendering part of the device in this work. Even though simple haptic effects already demonstrated the expressiveness of PneuSleeve, future works could study multi-sensory integration and explore how the haptic cues in different variants can be combined with visual and audio cues to further enhance user experience. User attention and perception to haptic feedback varies in mobile and on-the-go settings which may affect the detection thresholds as well as the recognition of feel effects. An analysis of PneuSleeve style haptic feedback for mobile augmented reality usecases will be useful.

Although the noise for most haptics effects in our study can be barely heard without headphones, some high frequency operations certainly produce some noise. In our user studies, we asked participants to notify the experimenter if noise were noticeable when they wore noise-canceling headphones playing pink noise at a pleasant volume. None of the participants mentioned about the noise during any of the experiments. This shows that the use of this type of regulator and muffler arrangement was sufficient for the purpose of the studies performed in this paper. For applications without headphones, high frequency noise can be further reduced by using a more advanced and customized muffler design. Other sound engineering methods, such as soundproofing foams, can be added around the regulators to further reduce the noise level.

CONCLUSION
We have introduced PneuSleeve, a soft, compact, and expressive haptic forearm sleeve. We used pneumatic pressure inside embroidered stretchable tubes to generate compression, skin stretch, and vibration, haptic stimuli. We have presented the design, construction, actuation and sensing mechanisms, and the implementation of the closed-loop compression force controller. Physical experimental results validated the performance of the actuators, sensors, and performance of the controller. Psychophysical experimental results validated the quantitative perceptibility and sensitivity of the haptic stimuli. Subjective experimental results showed that the renderable haptic stimuli can present a wide range of interesting effects to the user. PneuSleeve is a new approach for soft wearable haptic interfaces.

REFERENCES
[1] Nathaniel Agharese, Tyler Cloyd, Laura H Blumenschein, Michael Raitor, Elliot W Hawkes, Heather Culbertson, and Allison M Okamura. 2018. HapWRAP: Soft growing wearable haptic device. In *2018 IEEE International Conference on Robotics and Automation (ICRA)*. IEEE, 1–5.

[2] Faisal Arafsha, Kazi Masudul Alam, and Abdulmotaleb El Saddik. 2012. EmoJacket: Consumer centric wearable affective jacket to enhance emotional immersion. In *2012 international conference on innovations in information technology (IIT)*. IEEE, 350–355.

[3] Karlin Bark, Jason Wheeler, Gayle Lee, Joan Savall, and Mark Cutkosky. 2009. A wearable skin stretch device for haptic feedback. In *World Haptics 2009-Third Joint EuroHaptics conference and Symposium on Haptic Interfaces for Virtual Environment and Teleoperator Systems*. IEEE, 464–469.

[4] Alexandra Delazio, Ken Nakagaki, Roberta L Klatzky, Scott E Hudson, Jill Fain Lehman, and Alanson P Sample. 2018. Force jacket: Pneumatically-actuated jacket for embodied haptic experiences. In *Proceedings*

of the 2018 CHI Conference on Human Factors in Computing Systems. ACM, 320.

[5] Esther W Foo, J Walter Lee, Crystal Compton, Simon Ozbek, and Brad Holschuh. 2019. User experiences of garment-based dynamic compression for novel haptic applications. In *Proceedings of the 23rd International Symposium on Wearable Computers*. ACM, 54–59.

[6] MM Gavrilović and MR Marić. 1969. Positional servo-mechanism activated by artificial muscles. *Medical and Biological Engineering* 7, 1 (1969), 77–82.

[7] Aakar Gupta, Antony Albert Raj Irudayaraj, and Ravin Balakrishnan. 2017. HapticClench: Investigating Squeeze Sensations using Memory Alloys. In *Proceedings of the 30th Annual ACM Symposium on User Interface Software and Technology*. ACM, 109–117.

[8] Nur Al-huda Hamdan, Adrian Wagner, Simon Voelker, Jürgen Steimle, and Jan Borchers. 2019. Springlets: Expressive, Flexible and Silent On-Skin Tactile Interfaces. In *Proceedings of the 2019 CHI Conference on Human Factors in Computing Systems*. ACM, 488.

[9] Elliot W Hawkes, David L Christensen, and Allison M Okamura. 2016. Design and implementation of a 300% strain soft artificial muscle. In *2016 IEEE International Conference on Robotics and Automation (ICRA)*. IEEE, 4022–4029.

[10] Ronan Hinchet, Velko Vechev, Herbert Shea, and Otmar Hilliges. 2018. DextrES: Wearable Haptic Feedback for Grasping in VR via a Thin Form-Factor Electrostatic Brake. In *The 31st Annual ACM Symposium on User Interface Software and Technology*. ACM, 901–912.

[11] Da-Yuan Huang, Ruizhen Guo, Jun Gong, Jingxian Wang, John Graham, De-Nian Yang, and Xing-Dong Yang. 2017. RetroShape: Leveraging rear-surface shape displays for 2.5 D interaction on smartwatches. In *Proceedings of the 30th Annual ACM Symposium on User Interface Software and Technology*. ACM, 539–551.

[12] Alexandra Ion, Edward Jay Wang, and Patrick Baudisch. 2015. Skin drag displays: Dragging a physical tactor across the user's skin produces a stronger tactile stimulus than vibrotactile. In *Proceedings of the 33rd Annual ACM Conference on Human Factors in Computing Systems*. ACM, 2501–2504.

[13] Ali Israr and Ivan Poupyrev. 2011. Tactile brush: drawing on skin with a tactile grid display. In *Proceedings of the SIGCHI Conference on Human Factors in Computing Systems*. ACM, 2019–2028.

[14] Ali Israr, Siyan Zhao, Kaitlyn Schwalje, Roberta Klatzky, and Jill Lehman. 2014. Feel Effects: Enriching Storytelling with Haptic Feedback. *ACM Trans. Appl. Percept.* 11, 3 (Sept. 2014). DOI:
http://dx.doi.org/10.1145/2641570

[15] Claudio Pacchierotti, Stephen Sinclair, Massimiliano Solazzi, Antonio Frisoli, Vincent Hayward, and Domenico Prattichizzo. 2017. Wearable haptic systems for the fingertip and the hand: taxonomy, review, and perspectives. *IEEE transactions on haptics* 10, 4 (2017), 580–600.

[16] Roshan Lalitha Peiris, Yuan-Ling Feng, Liwei Chan, and Kouta Minamizawa. 2019. ThermalBracelet: Exploring Thermal Haptic Feedback Around the Wrist. In *Proceedings of the 2019 CHI Conference on Human Factors in Computing Systems*. ACM, 170.

[17] Evan Pezent, Ali Israr, Majed Samad, Shea Robinson, Priyanshu Agarwal, Hrvoje Benko, and Nick Colonnese. 2019. Tasbi: Multisensory squeeze and vibrotactile wrist haptics for augmented and virtual reality. In *2019 IEEE World Haptics Conference (WHC)*. IEEE, 1–6.

[18] Henning Pohl, Peter Brandes, Hung Ngo Quang, and Michael Rohs. 2017. Squeezeback: pneumatic compression for notifications. In *Proceedings of the 2017 CHI Conference on Human Factors in Computing Systems*. ACM, 5318–5330.

[19] Panagiotis Polygerinos, Zheng Wang, Kevin C Galloway, Robert J Wood, and Conor J Walsh. 2015. Soft robotic glove for combined assistance and at-home rehabilitation. *Robotics and Autonomous Systems* 73 (2015), 135–143.

[20] Domenico Prattichizzo, Francesco Chinello, Claudio Pacchierotti, and Monica Malvezzi. 2013. Towards wearability in fingertip haptics: a 3-dof wearable device for cutaneous force feedback. *IEEE Transactions on Haptics* 6, 4 (2013), 506–516.

[21] Michael Raitor, Julie M Walker, Allison M Okamura, and Heather Culbertson. 2017. WRAP: Wearable, restricted-aperture pneumatics for haptic guidance. In *2017 IEEE International Conference on Robotics and Automation (ICRA)*. IEEE, 427–432.

[22] Samuel B Schorr and Allison M Okamura. 2017. Fingertip tactile devices for virtual object manipulation and exploration. In *Proceedings of the 2017 CHI Conference on Human Factors in Computing Systems*. ACM, 3115–3119.

[23] HF Schulte Jr. 1961. The characteristics of the McKibben artificial muscle (1961) The Application of external power in prosthetics and orthotics. *National Academy of Sciences-National Research Council, Washington DC, Appendix H* (1961), 94–115.

[24] Youngbo Aram Shim, Jaeyeon Lee, and Geehyuk Lee. 2018. Exploring Multimodal Watch-back Tactile Display using Wind and Vibration. In *Proceedings of the 2018 CHI Conference on Human Factors in Computing Systems*. ACM, 132.

[25] Evan Strasnick, Jessica R Cauchard, and James A Landay. 2017. Brushtouch: Exploring an alternative tactile method for wearable haptics. In *Proceedings of the 2017 CHI Conference on Human Factors in Computing Systems*. ACM, 3120–3125.

[26] Nobuhiro Takahashi, Hayato Takahashi, and Hideki Koike. 2019. Soft Exoskeleton Glove Enabling Force

Feedback for Human-Like Finger Posture Control with 20 Degrees of Freedom. In *2019 IEEE World Haptics Conference (WHC)*. IEEE, 217–222.

[27] Fei Tang, Ryan P McMahan, and Tandra T Allen. 2014. Development of a low-cost tactile sleeve for autism intervention. In *2014 IEEE International Symposium on Haptic, Audio and Visual Environments and Games (HAVE) Proceedings*. IEEE, 35–40.

[28] Michael Wehner, Michael T Tolley, Yiğit Mengüç, Yong-Lae Park, Annan Mozeika, Ye Ding, Cagdas Onal, Robert F Shepherd, George M Whitesides, and Robert J Wood. 2014. Pneumatic energy sources for autonomous and wearable soft robotics. *Soft robotics* 1, 4 (2014), 263–274.

[29] Eric Whitmire, Hrvoje Benko, Christian Holz, Eyal Ofek, and Mike Sinclair. 2018. Haptic revolver: Touch, shear, texture, and shape rendering on a reconfigurable virtual reality controller. In *Proceedings of the 2018 CHI Conference on Human Factors in Computing Systems*. ACM, 86.

[30] Weicheng Wu and Heather Culbertson. 2019. Wearable Haptic Pneumatic Device for Creating the Illusion of Lateral Motion on the Arm. In *2019 IEEE World Haptics Conference (WHC)*. IEEE, 193–198.

[31] Eric M Young, Amirhossein H Memar, Priyanshu Agarwal, and Nick Colonnese. 2019. Bellowband: A Pneumatic Wristband for Delivering Local Pressure and Vibration. In *2019 IEEE World Haptics Conference (WHC)*. IEEE, 55–60.

[32] Mengjia Zhu, Thanh Nho Do, Elliot Hawkes, and Yon Visell. 2019. Fluidic Fabric Muscle Sheets for Wearable and Soft Robotics. *arXiv preprint arXiv:1903.08253* (2019).

[33] Bengang Zhuo, Sujie Chen, Mingmin Zhao, and Xiaojun Guo. 2017. High sensitivity flexible capacitive pressure sensor using polydimethylsiloxane elastomer dielectric layer micro-structured by 3-D printed mold. *IEEE Journal of the Electron Devices Society* 5, 3 (2017), 219–223.